Fractional Resonances between Waves and Energetic Particles in Tokamak Plasmas

G. J. Kramer,[1] L. Chen,[2,3] R. K. Fisher,[4] W. W. Heidbrink,[2] R. Nazikian,[1] D. C. Pace,[4] and M. A. Van Zeeland[4]

[1]*Princeton Plasma Physics Laboratories, P.O. Box 451, Princeton, New Jersey 08543, USA*
[2]*University of California-Irvine, Irvine, California 92697, USA*
[3]*Institute for Fusion Theory and Simulation, Zhejiang University, Hangzhou, 310027 China*
[4]*General Atomics, P.O. Box 85608, San Diego, California 92186, USA*

(Received 5 March 2012; published 18 July 2012)

From numerical simulation and analytical modeling it is shown that fast ions can resonate with plasma waves at fractional values of the particle drift-orbit transit frequency when the plasma wave amplitude is sufficiently large. The fractional resonances, which are caused by a nonlinear interaction between the particle orbit and the wave, give rise to an increased density of resonances in phase space which reduces the threshold for stochastic transport. The effects of the fractional resonances on spatial and energy transport are illustrated for an energetic particle geodesic acoustic mode but they apply equally well to other types of MHD activity.

DOI: 10.1103/PhysRevLett.109.035003 PACS numbers: 52.20.Dq, 52.25.Fi, 52.35.Fp, 52.35.Mw

Resonant interactions between waves and particles are ubiquitous in the physical world. Resonances between waves and drift-orbit transit frequencies of fast particles in magnetized plasmas play an important role in fast-ion transport and mode excitation. The well known linear resonance condition in tokamaks between a wave with frequency ω and the particle poloidal drift-orbit transit frequency, ω_t, is given by $\omega = p\omega_t + n\omega_\phi$ with n the toroidal mode number of the wave, ω_ϕ the toroidal transit frequency, and p the bounce harmonic number which is an integer in this expression [1–3]. In this Letter, however, we show that resonances between waves and particles can also occur when p is fractional. This increases the number of available wave-particle resonances significantly, and we explore the effects of fractional resonances on fast-ion transport. Although fractional resonances in nonlinear plasma media have been noticed previously [4,5], this Letter is the first to show that fractional resonances can cause particle losses in a magnetic confinement device. The fractional wave-particle resonances were first found in simulations of particles interacting with an energetic particle geodesic acoustic mode (E-GAM) [6], and they can be explained with a theoretical model presented in this Letter. The fractional resonances are not restricted to E-GAMs but they also appear when other MHD activity is present such as Alfvén eigenmodes at realistic mode amplitudes.

Wave-particle interactions can be studied in detail for the E-GAM because it is a global toroidally symmetric ($n = 0$) electrostatic mode with mode frequencies in the range of 10 to 30 kHz. It can be excited to large amplitudes: density fluctuations of $\tilde{n}/n \approx 10\%$ have been found experimentally [7] and can expel large numbers of fast ions. In accordance with Ref. [6] we have modeled the E-GAM as a time-varying electrostatic potential [Fig. 1(a)] which is a flux function. From this potential the radial electric field in the plasma was obtained [Fig. 1(d)]. The magnitude of the potential in the plasma center, 5 kV, was obtained by comparing the measured density fluctuations with the ones obtained from the displacement induced by the mode [7].

The full orbit following code SPIRAL [8], which calculates single particle orbits in toroidal geometry by solving the Lorentz equations, was used to calculate particle trajectories in the plasma in the presence of the E-GAM. Periodic excursions of the particle orbit and energy were found under the influence of a 15 kHz E-GAM with a central electrical potential of 5 kV as shown in Fig. 1 for a 50 keV deuteron launched on a passing orbit. Initially, the particle gains energy from the mode until its orbit becomes so large that the phase between the mode changes and the particle loses energy to the mode until it returns to its initial position and the whole process repeats itself.

In order to determine the resonances between the poloidal transit frequencies of the particles and a 15 kHz E-GAM we have launched a number of deuterons with energies between 5 and 150 keV with an initial pitch $(v_\parallel/v)$ of 0.5 at a major radius of 2.02 m at the midplane. The selected energy range gives poloidal transit frequencies between 4 and 40 kHz. For each particle the maximum and minimum energy excursion was determined and plotted against the initial transit frequency for a number of values of the central electrical potential as shown in Fig. 2.

At the lowest mode amplitude ($V_{\text{central}} = 0.005$ kV which is 0.1% of typical E-GAM amplitudes) only the linear $p = 1$, 2, and 3 resonances are visible. When the mode amplitude is increased to $V_{\text{central}} = 0.5$ kV several fractional resonances appear between the $p = 1$ and 2 resonances while at 30 kHz the $1/2$ resonance appears. The increased mode amplitude also broadens the resonances. This can be explained by the large excursions that the particle makes at those mode amplitudes. The time-averaged bounce

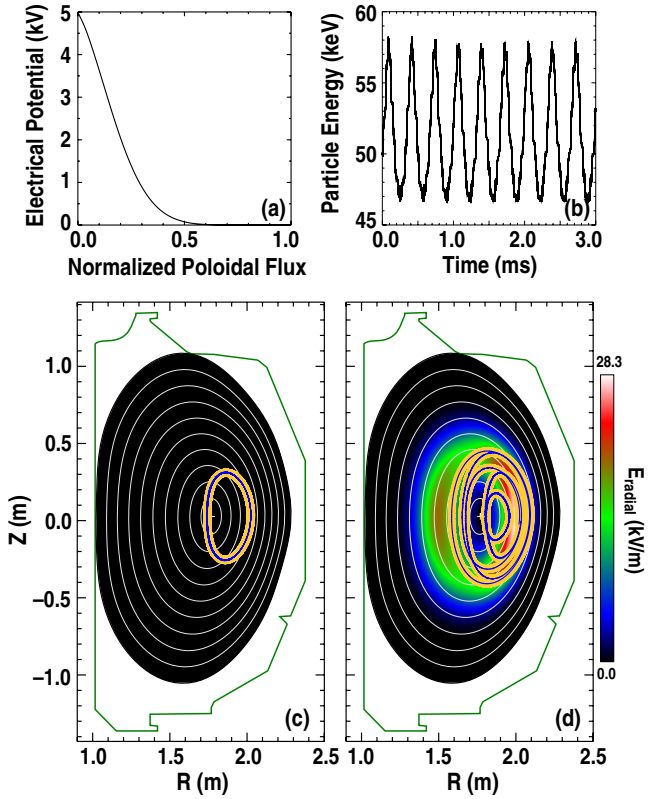

FIG. 1 (color online). (a) E-GAM potential. (b) Energy excursion of a 50 keV deuteron launched at $R = 2.02$ m and $Z = 0.0$ m, and at a pitch of 0.5, as a function of time in the presence of a 15 kHz E-GAM. The particle orbit during one energy cycle (0.33 ms) (c) without and (d) with the E-GAM present. Black (orange online) line: full orbit; light gray (blue online) line: guiding center.

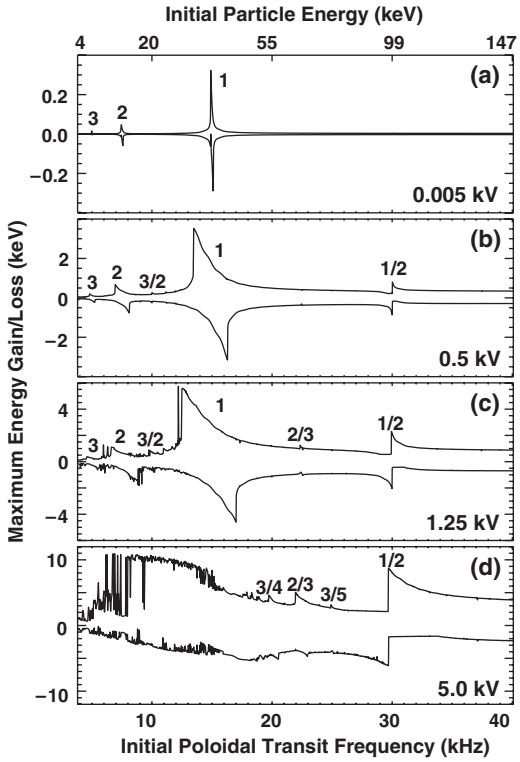

FIG. 2. Minimum and maximum particle energy excursion as a function of the initial transit frequency for various values of the electrical potential of the E-GAM. (a) At 0.05 kV only the linear resonances are present. (b) At 0.5 kV fractional resonances appear. (c) At 1.25 keV the threshold for mode overlap between linear and fractional resonances is passed, while (d) at 5 keV the region up to the fundamental resonance has become stochastic and subharmonic resonances are developing strongly. Integer and a number of fractional resonances are indicated.

period over one energy excursion cycle is now resonant with the mode frequency. At a central potential of 1.25 kV the threshold for resonance overlap between the linear and fractional resonances is passed as can be inferred from the spikes appearing in the energy traces near the the linear resonances. Finally, at $V_{\text{central}} = 5$ kV, the experimental value of the central potential, the orbits in the frequency interval up to the $p = 1$ resonance have become fully stochastic due to resonance overlap while at higher frequencies additional new subharmonic resonances have appeared.

The fractional resonances found in the simulations can be understood by writing down the Hamiltonian, $H = \varepsilon + e\delta\Phi$, of a charged particle with charge e, and kinetic energy, ε, in a time-varying electrical potential: $\delta\Phi = \Phi_0 \sin(\omega t - k_r r)$ with ω the mode frequency and k_r its wave number. Resonances correspond to secular behavior and are obtained when $\langle dH/dt \rangle \neq 0$ with $\langle \cdots \rangle = \frac{1}{T}\int_0^T \cdots dt$ and T the fast time scale. The unperturbed particle position is given by $r = r_0 + \rho_0$ with r_0 the drift center and ρ_0 the drift-orbit radius, and its radial drift velocity is $\dot{\rho}_0 = v_{dr} = v_d \sin(\theta)$. The angle coordinate, θ, and particle transit frequency, $\dot{\theta} = \omega_t$, are both functions of particle energy, pitch, and drift center. The mode induces a perturbation to the energy, $\varepsilon = \varepsilon_0 + \delta\varepsilon$, and drift center, $r_c = r_0 + \delta r$, whereby the effects in energy dominate over the change in drift-orbit center. The change of energy in time, given by $\delta\dot{\varepsilon} = v_{dr} e \delta E$ (δE is the electric field associated with the potential $\delta\Phi$), can be cast

$$\delta\dot{\varepsilon} = \frac{k_r v_{d0} e \Phi_0}{2} \sin[\theta_0 \pm (\omega t - k_r r)],$$

where the $\pm$ sign accounts for the fact that the mode forms beat waves with the particle transit frequency at the sum and difference frequency. The change of energy over time

$$\delta\varepsilon = \frac{k_r v_{d0} e \Phi_0}{2} \frac{\cos[\theta_0 \pm (\omega t - k_r r)] - \cos(\mp k_r r)}{\omega_{t0} \pm \omega}$$

can be obtained from a simple integration over time and by using the leading term of the particle transit frequency: $\dot{\theta}_0 = \omega_{t0}$. The next step is to expand the perturbed particle transit frequency as $\dot{\theta} = \omega_{t0} + (d_\varepsilon \omega_{t0})\delta\varepsilon + (d_r \omega_{t0})\delta r$

TABLE I. Coefficients used in Eqs. (1) and (2).

i	z_i	α_i	index
1	$-\frac{v_{d0}}{\omega_{t0}}$	$\omega_{t0}t$	j
2	$\left(\frac{k_r v_{d0} e\Phi}{4}\right)\left(v'_{d\varepsilon} - \frac{v_{d0}\omega'_{t\varepsilon}}{\omega_{t0}}\right)\left(\frac{4\omega^2 - 28\omega_{t0}^2}{(4\omega_{t0}^2-\omega^2)(\omega_{t0}^2-\omega^2)}\right)$	$k_r r$	k
3, 4	$\left(\frac{k_r v_{d0} e\Phi}{4}\right)\left(v'_{d\varepsilon} - \frac{v_{d0}\omega'_{t\varepsilon}}{\omega_{t0}}\right)\left(\frac{2}{(\omega_{t0}^2-\omega^2)}\right)$	$\omega_{t0}t \pm k_r r$	l, m
5	$\left(\frac{k_r v_{d0} e\Phi}{4}\right)\left(\frac{2v'_{d\varepsilon}}{\omega_{t0}^2-\omega^2} - \frac{4\omega_{t0} v_{d0}\omega'_{t\varepsilon}}{(\omega_{t0}^2-\omega^2)^2}\right)$	$\omega t - k_r r$	n
6, 7	$\left(\frac{k_r v_{d0} e\Phi}{4}\right)\left(\frac{v'_{d\varepsilon}}{(2\omega_{t0}\pm\omega)(\omega_{t0}\pm\omega)} + \frac{v_{d0}\omega'_{t\varepsilon}}{(2\omega_{t0}\pm\omega)(\omega_{t0}\pm\omega)^2}\right)$	$(2\omega_{t0} \pm \omega)t \mp k_r r$	p, q

(where $d_x y \equiv dy/dx$). Integrating this expression with time gives $\theta_0 = \omega_{t0}t$ for the first term and $\delta\theta = d_\varepsilon \omega_{t0} \int \delta\varepsilon dt$ for the second term while the third term is omitted because δr is small. In a similar manner the change in the drift-orbit radius is calculated as $\dot{\rho} = v_d \sin(\theta) = [v_{d0} + (d_\varepsilon v_{d0})\delta\varepsilon + (d_r v_{d0})\delta r]\sin(\theta_0 + \delta\theta)$ with $\dot{\rho} = \dot{\rho}_0 + \delta\dot{\rho}$, where $\dot{\rho}_0 = v_{d0}\sin(\theta_0)$ and $\delta\dot{\rho} = [(d_\varepsilon v_{d0})\delta\varepsilon + (d_r v_{d0})\delta r]\sin(\theta_0) + v_{d0}\cos(\theta_0)\delta\theta$. Integrating over time gives $\rho_0 = -v_{d0}\cos(\theta_0)/\omega_{t0}$, while $\delta\rho$ is evaluated as

$$\delta\rho = \sum_{i=2}^{7} z_i \cos(\alpha_i), \tag{1}$$

where z_i and α_i are given in Table I. Wave-particle resonances are now obtained from $\langle dH/dt\rangle = \omega e\Phi_0 \mathrm{Re}\langle e^{i[\omega t - k_r(r_c+\rho_0+\delta\rho)]}\rangle \neq 0$. The terms with ρ_0 and $\delta\rho$ contain cosine functions so we can use the Jacobi-Anger identity to express $\langle dH/dt\rangle$ as the product of Bessel functions (with $\psi = \omega t - k_r(r_c + \rho_0 + \delta\rho)$),

$$e^{i\psi} = \sum_{j,k,l,m,n,p,q} i^{j+2(k+l+q)} J_j(z_1)J_k(z_2)J_l(z_3)J_m(z_4)J_n(z_5)J_p(z_6)J_q(z_7) \times e^{i\{(k+l-m-n-p+q)k_r r + [(j+l+m+2(p+q))\omega_{t0} + (k+l-m+1)\omega]t - k_r r_c\}}, \tag{2}$$

where we have made use of the fact that $k + l - m - n - p + q = 0$, which must hold for the spatial part when the time average of this expression is nonzero. In a similar way the temporal part of Eq. (2) should be zero at the resonance, so we get

$$\frac{\omega}{\omega_{t0}} = -\frac{j + l + m + 2(p+q)}{(k + l - m + 1)}. \tag{3}$$

From this expression we can immediately see that a multitude of fractional resonances between the mode frequency, ω, and the initial particle transit frequency, ω_{t0}, are obtained with appropriate choices of the indices j, k, l, m, p, and q. The linear resonance condition is recovered when the potential, Φ, is vanishingly small and therefore k, l, m, p, and q are zero.

It is interesting to note the analogy between the fractional resonances and resonant heating below the cyclotron frequency as described in Refs. [9,10]. In the cyclotron case the heating, $\delta W_c = v_\perp e\delta E_\perp$, is caused by the product of the perpendicular velocity, $v_\perp$, and perpendicular electric field, $\delta E_\perp$ while the cyclotron frequency, ω_c, is constant. In the fractional resonances case the heating is given by $\delta\dot{\varepsilon} = v_{dr} e\delta E$, where v_{dr} plays the same role as $v_\perp$ in the cyclotron case, and the electric field, δE, is equivalent to $\delta E_\perp$. The particle transit frequency, ω_t, plays a similar role as ω_c but ω_t depends on the drift velocity. Another difference between the cyclotron and fractional resonances case is that the subharmonic resonances appear at frequencies below the fundamental cyclotron resonance while in the fractional resonances case the subharmonic resonances appear above the fundamental resonance [Fig. 2(a)].

The fractional resonances increase the resonance density in phase space as shown in Fig. 3. This can lead to

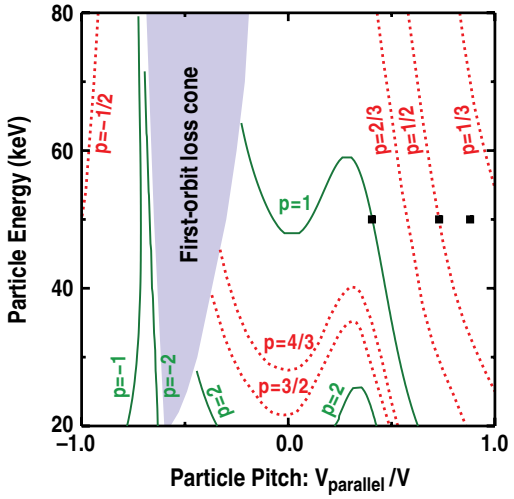

FIG. 3 (color online). Energy-pitch phase space with linear [solid (green online) line] and a small number of fractional resonances [dashed (red online) line] shown. The locations of the three ensembles that were used to investigate the effects of the fundamental resonance, the half resonance, and nonresonance on particle transport are indicated with the black squares.

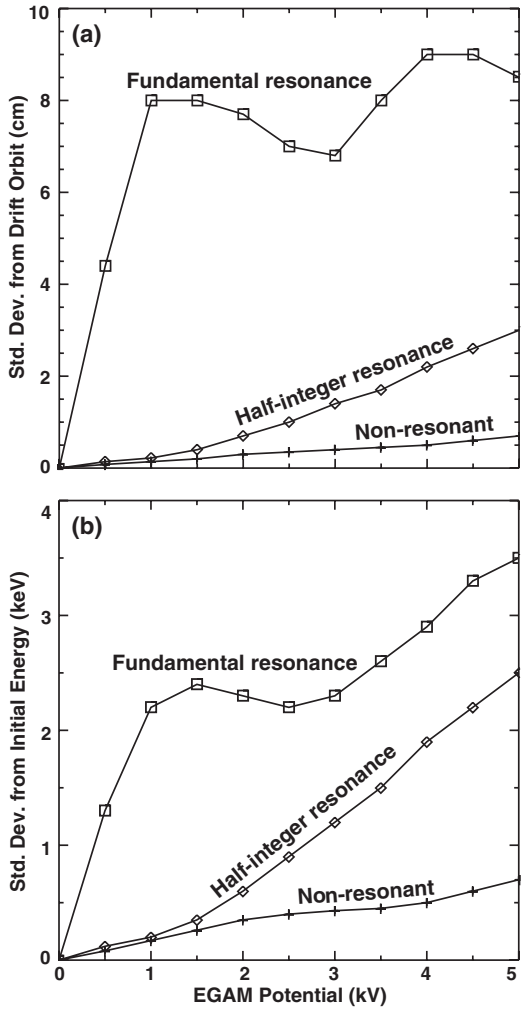

FIG. 4. Standard deviation of the (a) radial and (b) energy excursion of an ensemble of ions as a function of E-GAM mode amplitude for the fundamental resonance, the half resonance, and nonresonant particles.

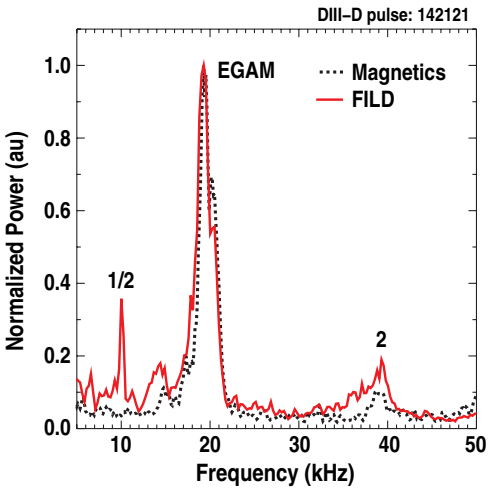

FIG. 5 (color online). Magnetic [dashed (black) line] and FILD [solid (red online) line] spectrum. Losses at half the E-GAM frequency are only observed with FILD.

increased transport in two ways: (i) stochastic transport can occur when the fractional and linear resonances overlap, while (ii) resonant transport can occur when the fractional resonances are well separated.

Stochastic transport occurs at sufficiently high mode amplitudes as can be seen in Fig. 2(d) where a stochastic region is formed below 18 kHz in the region where the linear resonances were located. The appearance of the fractional resonances between the linear resonances decreases the threshold for stochastic orbits. Another important observation that can be made from Fig. 2(d) is that when the region has become stochastic the particles gain more energy from the mode than that they lose to the mode which leads to a damping of the mode. In carefully designed experiments with cocurrent and countercurrent beam injection this damping may be observed experimentally.

Resonant transport was studied in simulations with three populations of 10 000 particles each with their guiding centers at $R, Z = (2.02, 0.0)$ m, an energy of 50 keV, and pitches of 0.40, 0.73, and 0.88, respectively, so that the particles are resonant with the fundamental resonance, resonant with the half resonance, and nonresonant, respectively, as indicated in Fig. 3 by the black squares. After the particles were distributed uniformly over the equilibrium drift orbit, the E-GAM was switched on for 0.27 ms and the spread in guiding centers relative to the unperturbed drift orbit and the spread in energy were calculated as a function of mode amplitude (Fig. 4).

From Fig. 4 it can be seen that the particles that were launched at the fundamental resonance are affected by very low wave amplitudes, which spread them in space and energy. The particle population at the half resonance is only affected when the mode amplitude reaches a threshold of 1 kV which is 20% of the amplitude seen in experiments. The nonresonant population is hardly affected by the mode. These results show clearly that the inclusion of the fractional resonances enhances the fast-ion transport and a larger part of phase space is affected by the mode than only the regions around the linear resonances.

Preliminary evidence of fast-ion transport at fractional harmonics of the mode frequency is observed during strong E-GAM activity in the DIII-D tokamak where the E-GAM was strongly excited during the current ramp-up phase with equal amounts (2.2 MW) of cocurrent and countercurrent neutral beam injection (NBI) similar to the experiments reported in Ref. [7] whereby the E-GAM is strongly driven by the countercurrent NBI (particle energy: 81 keV) while the cocurrent beam (particle energy: 76 keV) is injected in a region of phase space where the $p = 1/2$ resonance is residing (Fig. 3). In Fig. 5 the spectrum of E-GAM oscillations as measured with a Mirnov coil is compared with the spectrum of losses to a fast-ion detector (FILD) [11]. A peak in the loss spectrum occurs at the half harmonic that does not appear in the instabilities spectrum which is consistent

with the theoretical prediction that $\dot{\rho}$ should contain fractional harmonic oscillations at large mode amplitude.

From numerical simulation and analytical modeling it was found that fast ions can resonate with plasma waves at fractional values of the particle drift-orbit transit frequency when the plasma wave amplitude is sufficiently large. The fractional resonances, which are caused by a nonlinear interaction between the particle orbit and the wave, give rise to an increased density of resonances in phase space which reduces the threshold for stochastic fast-ion transport.

This work was supported by the U.S. Department of Energy under Awards No. DE-AC02-09CH11466, No. SC-G903402, and No. DE-FC02-04-ER54698. L. C. also acknowledges support by the ITER-CN Basic Research Programme.

[1] S. D. Pinches, V. G. Kiptily, S. E. Sharapov, D. S. Darrow, L.-G. Eriksson, H.-U. Fahrbach, M. García-Muñoz, M. Reich, E. Strumberger, A. Werner, ASDEX Upgrade Team, and JET-EFDA Contributors, Nucl. Fusion **46**, S904 (2006).

[2] W. W. Heidbrink, Phys. Plasmas **15**, 055501 (2008).

[3] M. García-Muñoz, H.-U. Fahrbach, S. D. Pinches, V. Bobkov, M. Brüdgam, M. Gobbin, S. Günter, V. Igochine, Ph. Lauber, M. J. Mantsinen, M. Maraschek, L. Marrelli, P. Martin, P. Piovesan, E. Poli, K. Sassenberg, G. Tardini, H. Zohm, and ASDEX Upgrade Team, Nucl. Fusion **49**, 085014 (2009).

[4] G. J. Lewak and C. S. Chen, J. Plasma Phys. **3**, 481 (1969).

[5] P. J. Peverly, R. E. Wagner, Q. Su, and R. Grobe, Laser Phys. **10**, 303 (2000).

[6] G. Y. Fu, Phys. Rev. Lett. **101**, 185002 (2008).

[7] R. Nazikian, G. Y. Fu, M. E. Austin, H. L. Berk, R. V. Budny, N. N. Gorelenkov, W. W. Heidbrink, C. T. Holcomb, G. J. Kramer, G. R. McKee, M. A. Makowski, W. M. Solomon, M. Shafer, E. J. Strait, and M. A. Van Zeeland, Phys. Rev. Lett. **101**, 185001 (2008).

[8] G. J. Kramer, R. B. White, R. Nazikian, and H. L. Berk, in *Proceedings of the 22nd International Fusion Energy Conference, Geneva, 2008*, http://www-pub.iaea.org/MTCD/Meetings/FEC2008/it_p6-3.pdf.

[9] L. Chen, Z. Lin, and R. White, Phys. Plasmas **8**, 4713 (2001).

[10] R. White, L. Chen, and Z. Lin, Phys. Plasmas **9**, 1890 (2002).

[11] R. K. Fisher, D. C. Pace, M. García-Muñoz, W. W. Heidbrink, C. M. Muscatello, M. A. Van Zeeland, and Y. B. Zhu, Rev. Sci. Instrum. **81**, 10D307 (2010).